AD-A133 338 FINITE GEOMETRY EFFECTS ON THE STABILITY OF A CHARGED BEAM PROPAGATING TH..(U) NAVAL RESEARCH LAB WASHINGTON DC G GANGULI ET AL. 28 SEP 83 NRL-MR-5191 1/1

UNCLASSIFIED F/G 20/7 NL

END
DATE
FILMED
10-83
DTIC

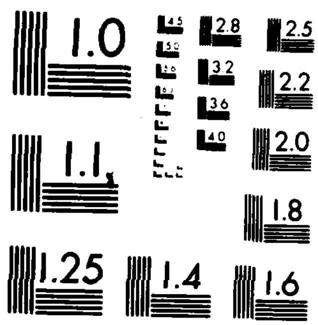

MICROCOPY RESOLUTION TEST CHART
NATIONAL BUREAU OF STANDARDS 1963-A

AD-A133 338

83 10 07 053

SECURITY CLASSIFICATION OF THIS PAGE (When Data Entered)

REPORT DOCUMENTATION PAGE	READ INSTRUCTIONS BEFORE COMPLETING FORM
1. REPORT NUMBER: NRL Memorandum Report 5191 — 2. GOVT ACCESSION NO.: AD-A133338	3. RECIPIENT'S CATALOG NUMBER
4. TITLE (and Subtitle): FINITE GEOMETRY EFFECTS ON THE STABILITY OF A CHARGED BEAM PROPAGATING THROUGH A RELATIVISTIC ANNULAR ELECTRON BEAM	5. TYPE OF REPORT & PERIOD COVERED: Interim report on a continuing NRL problem.
	6. PERFORMING ORG. REPORT NUMBER
7. AUTHOR(s): G. Ganguli* and P. Palmadesso	8. CONTRACT OR GRANT NUMBER(s)
9. PERFORMING ORGANIZATION NAME AND ADDRESS: Naval Research Laboratory, Washington, DC 20375	10. PROGRAM ELEMENT, PROJECT, TASK AREA & WORK UNIT NUMBERS: 61153N; RR033-02-44; 47-0884-0-3
11. CONTROLLING OFFICE NAME AND ADDRESS: Office of Naval Research, Arlington, VA 22203	12. REPORT DATE: September 28, 1983
	13. NUMBER OF PAGES: 22
14. MONITORING AGENCY NAME & ADDRESS (if different from Controlling Office)	15. SECURITY CLASS. (of this report): UNCLASSIFIED
	15a. DECLASSIFICATION/DOWNGRADING SCHEDULE

16. DISTRIBUTION STATEMENT (of this Report)

Approved for public release; distribution unlimited.

17. DISTRIBUTION STATEMENT (of the abstract entered in Block 20, if different from Report)

18. SUPPLEMENTARY NOTES

*Present address: Science Applications, Inc., McLean, VA 22102

This work was supported by the Office of Naval Research.

19. KEY WORDS (Continue on reverse side if necessary and identify by block number)

Electron acceleration
Collective acceleration
Relativistic beams

20. ABSTRACT (Continue on reverse side if necessary and identify by block number)

Finite geometry effects on the stability properties of a charged beam propagating through an intense relativistic annular electron beam has been studied. The stability of the system under transverse oscillation has been examined in detail in a parameter domain pertinent to the Collective Particle Accelerator, currently under development at the Naval Research Laboratory. Both the normal mode and the convective aspects of this instability have been investigated. Despite a substantial temporal growth rate as predicted by the normal mode approach this instability does not prevent successful acceleration of a portion of the axial beam. Thus the transverse oscillation is not fatal to the CPA operation.

DD FORM 1473, 1 JAN 73 — EDITION OF 1 NOV 65 IS OBSOLETE
S/N 0102-014-6601

SECURITY CLASSIFICATION OF THIS PAGE (When Data Entered)

CONTENTS

FINITE GEOMETRY EFFECTS ON THE STABII.ITY OF A CHARGED BEAM PROPAGATING THROUGH A RELATIVISTIC ANNULAR ELECTRON BEAM

I. Introduction

The stability properties of systems of intense relativistic electron beams are of considerable interest for many applications. The Collective Particle Accelerator (CPA), currently under development at the Naval Research Laboratory is one such application. The Collective Particle Accelerator is a device in which an intense modulated hollow electron beam propagates along a rippled magnetic field. The interaction of the modulated annular electron beam with the rippled magnetic field produces an axial electric field which consists of both backward and forward waves[1]. A solid electron beam can be introduced axially and entrapped by the backward wave potential. There is a transfer of energy from the axial electric field to the axial beam particles which in turn get accelerated to high energies, provided that both beams propagate in a stable fashion. In this paper we examine some stability properties of a solid charged beam propagating through an annular intense relativistic electron beam in the parameter domain pertinent to the Collective Particle Accelerator at the Naval Research Laboratory.

An earlier study[2] of the coupled transverse oscillation for an intense unmodulated charged particle beam in a straight guiding magnetic field concluded that the transverse oscillation excited by the propagation of a solid charged beam inside a hollow relativistic electron beam is unstable. The growth rate of this instability is a significant fraction of the diocotron frequency of the hollow beam for a solid electron beam and even greater if the solid beam is made up of ions. In this paper we study this instability more specifically in the context of the CPA. As in Ref. 2 we use a fluid model for the hollow electron beam and a kinetic model for the solid beam. In order to

Manuscript approved July 29, 1983.

make the analysis simple, here we ignore the ripples in the axial magnetic field and the beam modulation. The radius of the solid beam R_s is taken to be less than the inner radius R_1 of the hollow electron beam. In order to make this study more relevant to the experiments we have recognized the finite extent of the system in the axial direction. A rigorous study of a finite system involves a two dimensional eigenvalve equation and its solution. This is beyond the scope of this paper and will be addressed in a future paper. Here we solve the wave kinetic equation and show that a successful acceleration is always possible for the beam head. This is because the wave energy of the instability travels at the group velocity V_g which is much smaller than the beam velocity v, which in turn is close to the speed of light. Thus the transverse oscillation is not fatal for the CPA operation as was implied in Ref. 2.

The composition of this paper is as follows: In Section II we review the equilibrium properties, the basic assumptions and the equations governing the system. In section III we solve the dispersion relation in the parameter domain pertinent to the CPA at the Naval Research Laboratory and discuss the results for a solid electron beam. In Section IV we solve the wave kinetic equation and discuss its relevance to a finite device and finally in Section V we give our conclusions.

II. Theory:

The equilibrium configuration is given in figure (1). We follow the treatment as given in Ref. 2. An intense relativistic charged electron beam propagates along the axial magnetic field $B_o\hat{e}_z$. The inner radius of this annular beam is R_1 while the outer radius is R_2. A solid beam of radius R_s propogates along the magnetic field. The solid beam radius R_s is smaller than

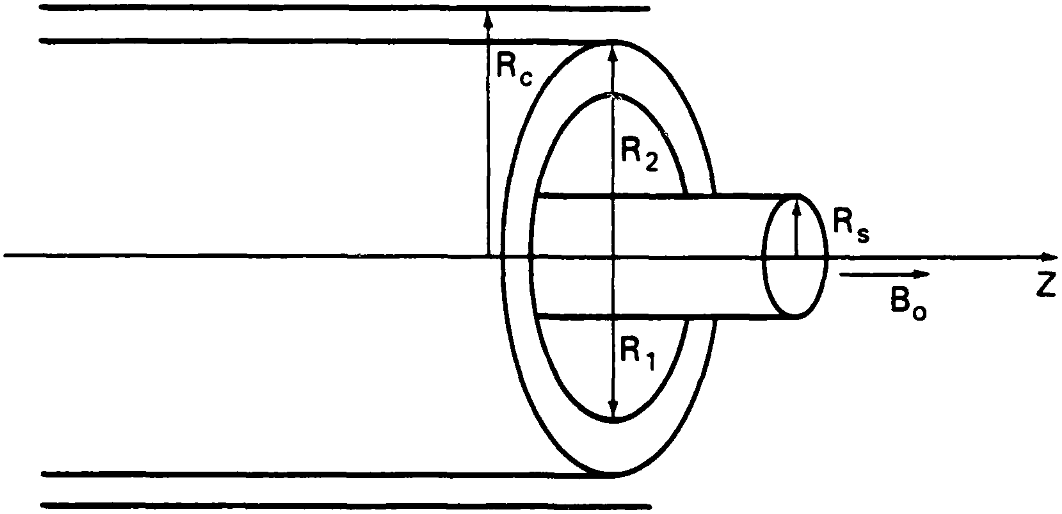

Figure 1a — The equilibrium configuration of the hollow and the solid beams.

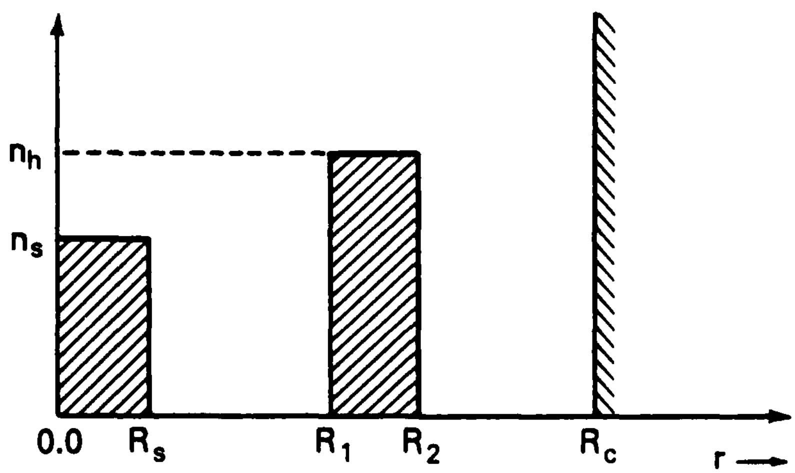

Figure 1b — The density profile for the equilibrium as shown in figure 1a.

the inner radius R_1 of the annular electron beam. The magnetic field confines the beams in the radial direction in equilibrium. Cylindrical coordinates (r,θ,z) is used.

We assume that the transverse velocities are much smaller than the axial velocity i.e., $v_z^2 >> v_r^2 + V_\theta^2$. The hollow beam is tenous $\omega_{ch}^2 >> \omega_{ph}^2$, where $\omega_{ph}^2 = 4\pi e^2 n_h/m_h$ and $\omega_{ch} = eB_o/\gamma_h m_h c$, $\gamma_h = (1-\beta_h^2)^{-1/2}$ and $\beta_h = v_h/c$. Further we assume that $\nu_s/\gamma_s = N_s Z_s^2 e^2/m_s c^2 \gamma_s << 1$, where s denotes the solid beam particles, ν_s is Budker's parameter, $N_s = 2\pi \int_o^{2\pi} dr\, r n_s^o(r)$ is the number of particles per unit axial length, $n_s^o(r)$ is the equilibrium particle density, $-e$ is the electron charge, Z_s is the charge state of the solid beam particles, $\gamma_s m_s c^2$ is the characteristic particle energy for the solid beam and c is the speed of light in vacuum. Since the axial velocity is much greater than the azimuthal velocities ($v_z^2 >> v_r^2 + v_\theta^2$) the self-magnetic field in the axial direction produced by the azimuthal current can be neglected. The equilibrium is azimuthally and axially symmetric i.e., $\frac{\partial}{\partial\theta} \equiv 0$ and $\frac{\partial}{\partial z} \equiv 0$.

The annular beam electrons are described as macroscopic, cold fluid immersed in an axial magnetic field $B_o\hat{e}_z$. The equation of motion and the continuity equation for the hollow beam electrons are

$$\left\{\frac{\partial}{\partial t} + \underline{V} \cdot\nabla\right\} \gamma_h m_h \underline{V} = -e \left\{\underline{E} + \frac{\underline{V} \times \underline{B}}{c}\right\}, \tag{1}$$

and

$$\frac{\partial}{\partial t} n_h + \nabla\cdot(n_h \underline{V}) = 0, \tag{2}$$

where $\underline{E}$ and $\underline{B}$ are the electric and the magnetic fields respectively, n_h and $\underline{V}$ are the density and the mean velocity, m_h is the rest mass of the annular beam particles (in this case the electrons).

The distribution function for the solid beam particles is given by

$$f_s^o(\underline{x},\underline{p}) = (n_s/2\pi\gamma_s m_s)\ \delta(H-\omega_s P_\theta - \hat{\gamma}_s m_s c^2)\ \delta(P_z-\gamma_s m_s \beta_s c) \qquad (3)$$

where n_s is the particle density at $r = 0$, $H = (m_s^2c^4 + c^2p^2)^{1/2} + e_s\Phi_o(r)$ is the total energy, $P_\theta = r[p_\theta + (e_s/c)\ (rB_o/2)]$ is the canonical angular momentum, $P_z = p_z + (e_s/c)\ A_z^o(r)$ is the axial canonical momentum, $A_z^o(r)$ is the axial component of the vector potential for the azimuthal self magnetic field, and ω_s, β_s and $\hat{\gamma}_s$, are constants. $\Phi_o(r)$ appearing in the definition of H is the electrostatic potential for the equilibrium self electric field.

The density profile consistent with the solid beam distribution is given by [3,2],

$$n_s^o(r) = \begin{cases} n_s, & 0 \leq r < R_s \\ o, & \text{otherwise.} \end{cases}$$

The fast (+) and the slow (-) laminar rotational frequencies are given by[2]

$$\omega_s^{\pm} = -\frac{\varepsilon_s}{2}\,\omega_{cs}\left[1 \pm \left(1 - \frac{2\omega_{ps}^2}{\gamma_s^2\,\omega_{cs}^2}\right)^{1/2}\right], \qquad (4)$$

where $\omega_{cs} = eZ_sB_o/\gamma_s m_s c$, $\omega_{ps}^2 = 4\pi n_s e^2\ Z_s^2/\gamma_s m_s$, $\gamma_s = (1-\beta_s^2)^{-1/2}$, $\beta_s = v_s/c$ and $\varepsilon_s = \mathrm{Sgn}\ (e_s)$. For a valid equilibrium for the solid beam ω_s is

restricted between $\omega_s^{\pm}$ i.e., $\omega_s^- < \omega_s < \omega_s^+$. The density profile for the annular beam electrons is given by,

$$n_h^o(r) = \begin{cases} n_h, & R_1 < r < R_2 \\ o, & \text{otherwise.} \end{cases}$$

The density profiles chosen here have sharp boundaries as shown is figure - 1b. Consistent with the equilibrium conditions just described the rotational frequency of the annular beam $\omega_h(r)$ is given by[2],

$$\omega_h(r) = \omega_D\left(1 - \frac{R_1^2}{r^2} - \gamma_h^2 \frac{\varepsilon_s n_s Z_s}{n_h}(1-\beta_s\beta_h)\frac{R_s^2}{r^2}\right), \tag{5}$$

where the diocotron frequency of the hollow beam is given by

$$\omega_D = \omega_{ph}^2/2\gamma_h^2\omega_{ch} \quad . \tag{6}$$

For the stability analysis for the coupled tranverse oscillation of an intense charged beam travelling through a relativistic annular electron beam, a normal mode approach is used. A dispersion relation is obtained by linearizing fluid, Vlasov and Maxwell's equations. All perturbations are assumed to vary in time and space as,

$$\delta\phi(\underline{x}, t) = \hat{\phi}(r)\exp[i(\ell\theta + kz - \omega t)], \tag{7}$$

where ω is the complex eigen frequency. The azimuthal harmonic number is ℓ and k is the axial wave vector. We further assume that the axial wavelength is long i.e.,

$$(kR_c)^2 \ll (\ell^2 + 1),$$

and the frequencies are low i.e.,

$$|\omega R_c|^2/c^2 \ll (\ell^2 + 1),$$

where R_c is the radius of the conducting wall.

Under these conditions the dispersion relation obtained by Uhm[2] is given by,

$$\Gamma_h(\omega,k)\ \Gamma_s(\omega,k) = \gamma_h^2\gamma_s^2\ (1-\beta_s\beta_h)^2\ \left(\frac{R_s}{R_1}\right)^{2\ell}\ \frac{S}{2\gamma_s^2}$$

$$\left[\frac{H(R_1)}{2\gamma_h^2}\ \left(1 - \frac{R_1^{\ 2\ell}}{R_c^{\ 2\ell}}\right)\ \left\{1 - \frac{R_1^{\ 2\ell}}{R_c^{\ 2\ell}} + \frac{H(R_2)}{2\gamma_h^2}\ \left(1 - \frac{R_1^{\ 2\ell}}{R_2^{\ 2\ell}}\right)\right.\right.$$

$$\left.\left.\left(1 - \frac{R_2^{\ 2\ell}}{R_c^{\ 2\ell}}\right)\right\} - \frac{H(R_2)}{2\gamma_h^{\ 2}}\ \frac{R_1^{\ 2\ell}}{R_2^{\ 2\ell}}\ \left(1 - \frac{R_2^{\ 2\ell}}{R_c^{\ 2\ell}}\right)\right]\ , \tag{8}$$

where the dielectric functions of the hollow and the solid beams are,

$$\Gamma_h\ (\omega,k) = \frac{H(R_1)}{2\gamma_h^{\ 2}}\ \left[1 - \frac{R_1^{\ 2\ell}}{R_c^{\ 2\ell}} + \frac{H(R_2)}{2\gamma_h^{\ 2}}\left(1 - \frac{R_1^{\ 2\ell}}{R_2^{\ 2\ell}}\right)\ \left(1 - \frac{R_2^{\ 2\ell}}{R_c^{\ 2\ell}}\right)\right]$$

$$- \frac{H(R_2)}{2\gamma_h^2}\ \left(1 - \frac{R_2^{\ 2\ell}}{R_c^{\ 2\ell}}\right) - 1, \tag{9}$$

$$\Gamma_s(\omega,k) = \frac{S}{2\gamma_s^2}\left(1 - \frac{R_s^{2\ell}}{R_c^{2\ell}}\right) - 1, \tag{10}$$

$$\frac{H(r)}{2\gamma_h^2} = \frac{\omega_D}{\omega - k\beta_h c - \ell\omega_h(r)}\ , \tag{11}$$

and

$$S = \frac{\omega_{ps}^2}{(\omega - k\beta_s c - \ell\omega_s)\left[(\omega - k\beta_s c - \ell\omega_s) + \varepsilon_s\omega_{cs} + 2\omega_s\right]}. \tag{12}$$

In the following sections of this paper we shall use the dispersion relation as given in equation (8) to examine the stability of the transverse oscillations for the NRL CPA. The details of the derivation of the dispersion relation are given in Ref. 2.

III. Results

In this section we solve the dispersion relation given in equation (8) in the parameter range pertinent to the NRL CPA. Here R_1 = 2.0625 cms, R_2 = 2.25 cms, R_s = 0.25cms and R_c = 2.3438cms. The injection energy of the hollow beam electrons is one MeV which corresponds to β_h = 0.941 while the injection energy of the solid beam electron is 0.7 MeV which gives $|\beta_s|$ = 0.906 . The space charge limiting current for the hollow beam is 20 kilo Amps and 2 kilo Amps for the solid beam giving the ratio I_s/I_h = 0.1. Given the ratio of the currents, the velocities and the areas of cross-section of the solid and the hollow beams, the ratio of the densities can be calculated. The expression for the density ratio for the solid and the hollow beams is,

$$\frac{n_s}{n_h} = \left(\frac{I_s}{I_h}\right)\left(\frac{\beta_h}{\beta_s}\right)\left(\frac{A_h}{A_s}\right), \tag{13}$$

where A_h and A_s are the areas of cross-section of the hollow and the solid beams respectively. In all the calculations given in this paper we have used the expression (13) for the density ratio and used $(\omega_{ph}/\omega_{ch})^2 = 0.1$.

In figure 2 we plot the real and the imaginary parts of the complex frequency ω against the axial wave vector k, for the azimuthal mode number $\ell = 1$. The instability exists roughly for kc/ω_D between -0.85 to 0.25, and achieves a maximum at $kc/\omega_D \sim -0.3$. The growth rate at its peak is about $0.5\omega_D$, which is a substantial fraction of the diocotron frequency of the hollow beam. The instability once again reappears in the range $0.55 < kc/\omega_D < 1.1$, but with much reduced temporal growth rate. This as explained by Uhm[2], is a residual influence of the familiar diocotron instability. Since the instability is a significant fraction of the diocotron frequency, Uhm[2] concluded that the propagation of the solid beam will be severely limited. In the following section we shall apply the finite geometry restriction in the axial direction and show that despite the substantial temporal growth rate it is possible to achieve successful acceleration.

In figure 3 we provide a plot of the maximized growth rate against the ratio of space charge limited currents (I_s/I_h) for the solid and the hollow beams. In this plot the ratio of the densities n_s/n_h, is calculated self consistently by equation (13). The values of the self consistent n_s/n_h are indicated on the plot at various values of I_s/I_h. The growth rate increases with increasing I_s/I_h. The ratio of the currents, I_s/I_h was varied from 0.01 to 0.2; and the corresponding maximized growth rate increased from $0.153\omega_D$ to $0.687\omega_D$. The self consistent density ratio n_s/n_h in the same range increased from 0.134 to 2.69. The value of kc/ω_D where the maximum occured moved from -0.15 to -0.45.

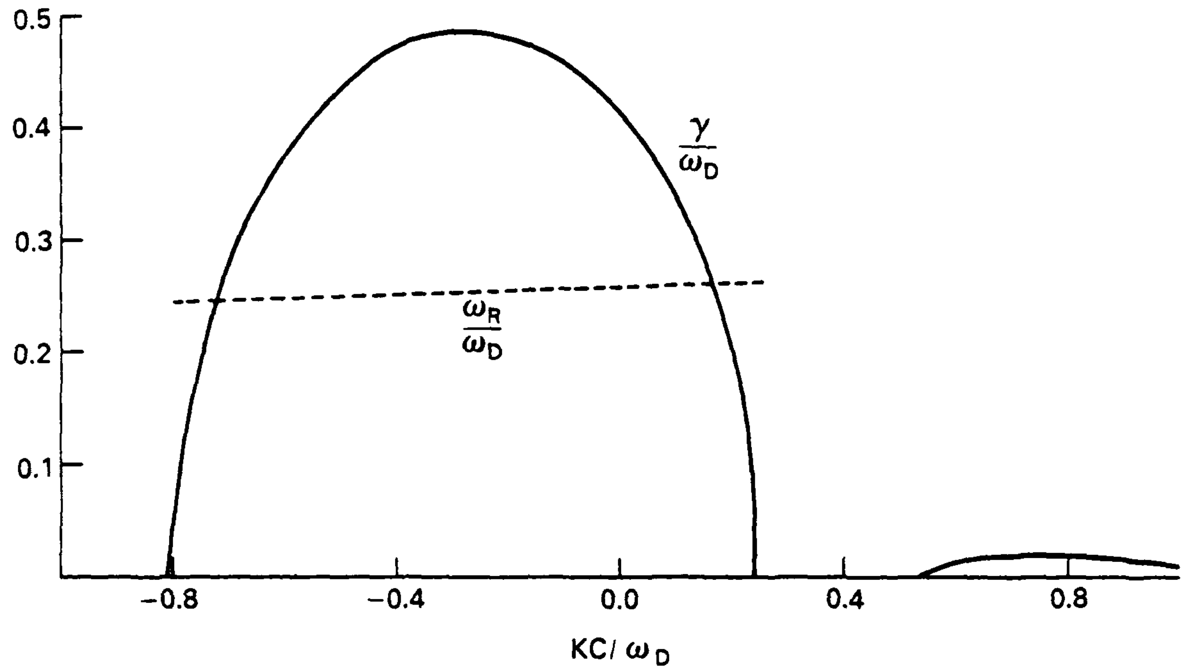

Figure 2 — A plot of the growth rate against the axial wave vector. Here R_1 = 2.0625 cms R_2 = 2.25 cms, R_s = 0.25 cms, R_c = 2.3438 cms. I_s/I_h = .1 and n_s/n_h is in accordance of equation (13). β_h = 0.941, β_s = 0.906 and the azimuthal wave number ℓ = 1 .

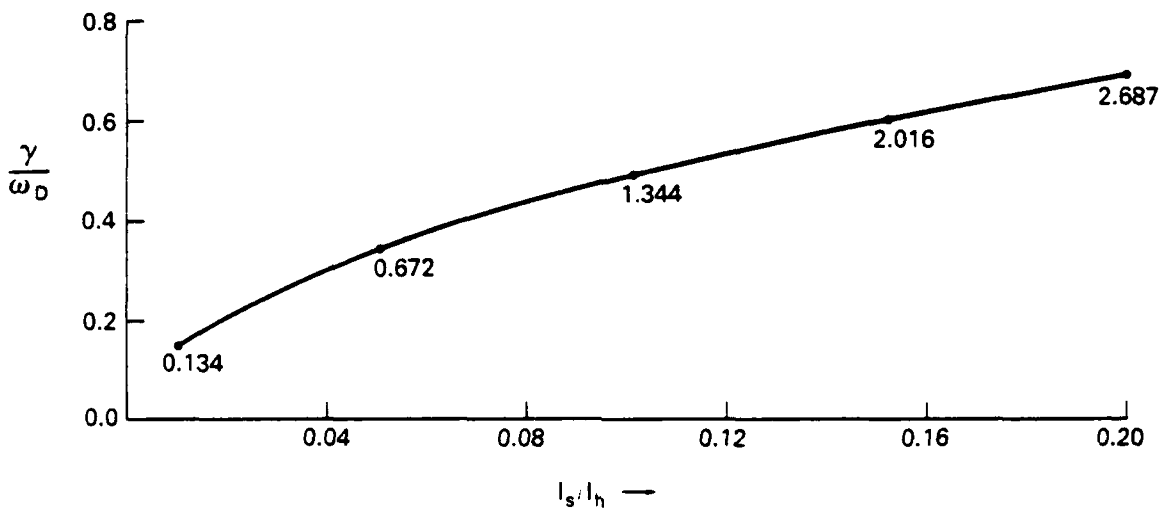

Figure 3 — A plot of the growth rates maximized over the axial wave vector as a function of the ratio of the space charge limited currents in the solid and the hollow beams. The density ratio n_s/n_h is computed self consistently by equation (13) and its magnitude for various I_s/I_h values are indicated on the plot.

Figure 4 is a plot of the maximized growth rate against the velocity of the solid beam β_s. Again the density ratio n_s/n_h is given by equation (13). We see that as β_s becomes small the density ratio n_s/n_h increases thereby increasing the growth rates. Since in the NRL experiment β_s for a solid electron beam is always in the opposite direction of the hollow electron beam velocity $\beta_h c$, we have restricted our calculations only to negative values of β_s. For $\beta_s < -0.5$ the growth rate becomes more or less constant. This is unlike the nature indicated in the figure 2 of Ref. 2, where n_s/n_h is held constant throughout the range of β_s. Hence the figure 2 of Ref. 2 does not correspond to one particular experimental setup. If we set $\beta_s = \beta_h$, i.e. consider the case where both the hollow beam and the solid beam travels at the same speed the growth rate vanishes.

IV. Finite Geometry Effects:

In the previous section we have shown that a solid electron beam propagating through a relativistic hollow electron beam is unstable to the transverse oscillation. This was the primary reason which lead Uhm[2] to conclude that the propagation of the solid beam through a hollow relativistic electron beam will be severely limited. In this section we shall study the propagation of the energy density W due to the instability along with the propagation of the beam head itself for finite systems.

The wave kinetic equation for the CPA is,

$$\frac{\partial W}{\partial t} + V_g \frac{\partial W}{\partial z} = \gamma W[1 - H(z-\beta_s ct)], \tag{14}$$

where W is the energy density, V_g is the group velocity of the transverse mode, $H(z-\beta_s ct)$ is the Heavside step function,

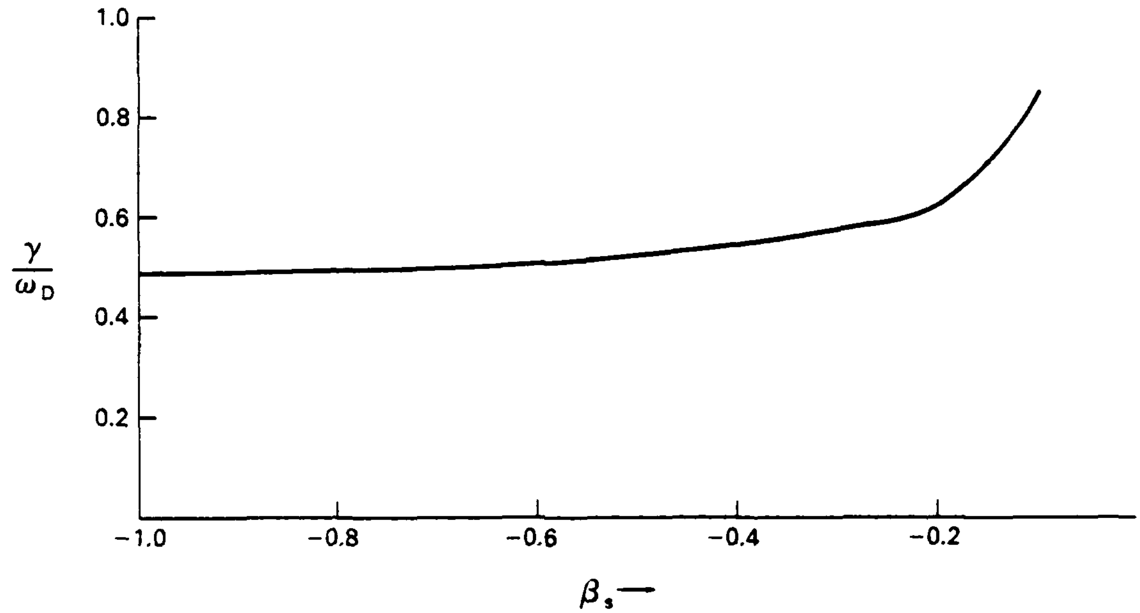

Figure 4 — A plot for the growth rate maximized over the axial wave vector k against the velocity of the solid beam β_s .

$$H(x) = \begin{cases} 1, & x>0 \\ 0, & \text{otherwise,} \end{cases}$$

and γ is the growth rate of the transverse instability. Fig (5) describes the CPA configuration. The annular beam propagates along the magnetic field $B_o\hat{e}_z$ between the radii R_1 and R_2. The solid beam propagates along the axis with a radius R_s and with a velocity $\beta_s c$. If the solid beam particles are electrons then the solid and the annular beam travel in the opposite direction while if the solid beam particles are ions then they travel in the same direction. The position of the beam head at any a time t is given by $\beta_s ct$.

First we shall discuss the case of a solid electron beam propagating through a relativistic hollow electron beam. The configuration is described in figure (5). The general solution of equation (14) can be written as,

$$W(\eta,z) = W_o\exp\left[\frac{\gamma}{V_g}\int_o^z \left\{1 - H\left(\left(1 - \frac{\beta_s c}{V_g}\right)z' + \frac{\beta_s c}{V_g}\eta\right)\right\}dz'\right] \tag{14a}$$

where,

$$\eta = z - V_g t$$

and

$$W_o = W(o,\eta) .$$

Define,

$$\hat{z} = \left(\frac{V}{V - V_g}\right)\eta, \tag{15}$$

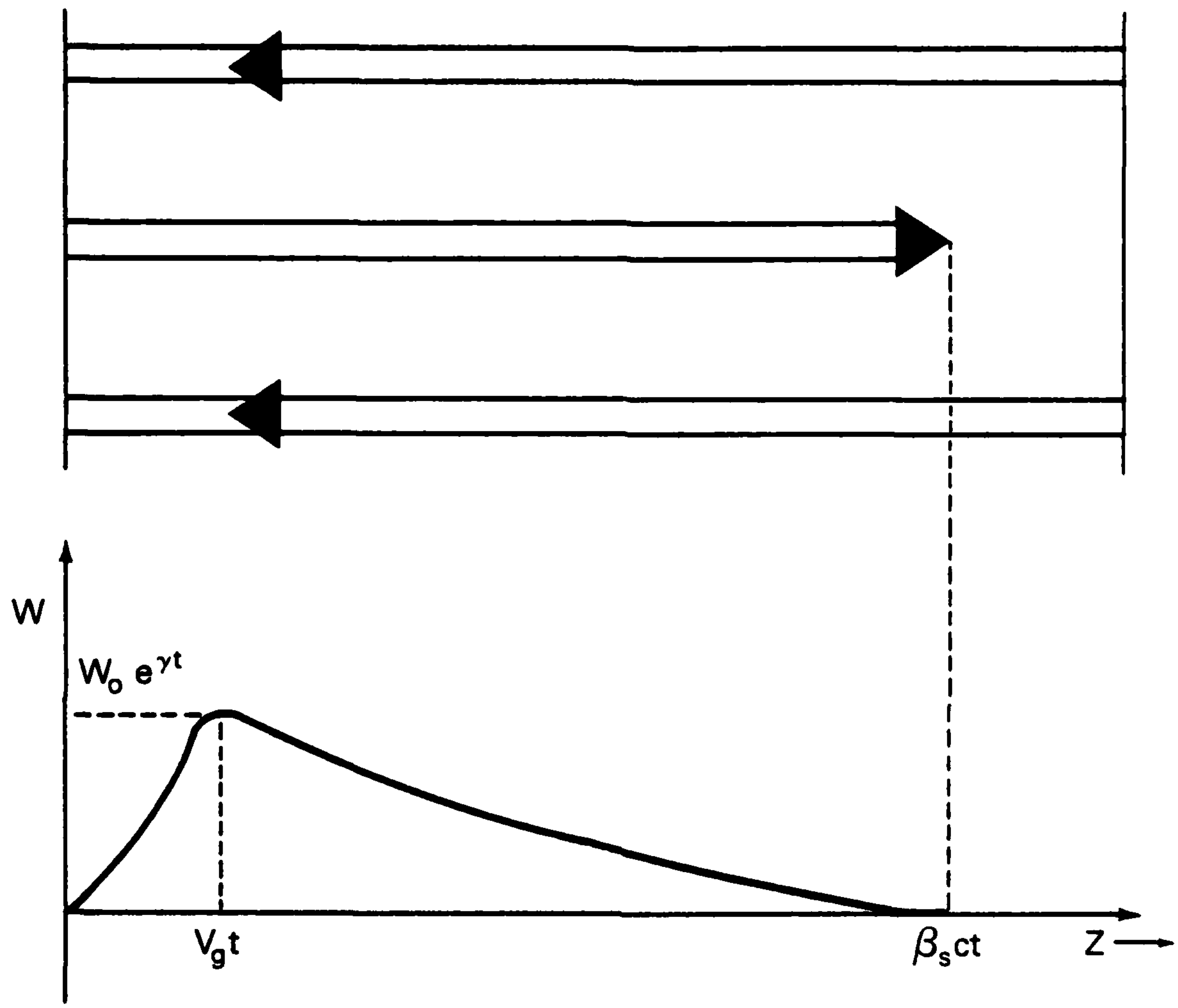

Figure 5 — A schematic diagram of the hollow electron beam and a solid electron beam. Also shown schematically is the solution $W(z,t)$ of equation (14) for this case.

such that

$$(1 - \frac{\beta_s c}{V_g})\hat{z} + \frac{\beta_s c}{V_g}\eta = 0 \ .$$

We shall discuss the solution (14a) in three regions:

(a) $\underline{z > \beta_s ct}$

This corresponds to the case of $\hat{z} > z$. For $\hat{z}>z$ the argument of H is positive and thus the solution becomes

$$W(z,t) = W_o \tag{16}$$

The solution implies that the energy of the region where the solid beam has not yet arrived remains unaffected at the initial value W_o.

(b) $\underline{V_g t \leq z \leq \beta_s ct}$

This corresponds to the case $0 < \hat{z} < z$. Here the solution is given by,

$$W(z,t) = W_o \exp\{\frac{\gamma}{\beta_s c - V_g}(\beta_s ct - z)\} \tag{17}$$

At $z = \beta_s ct$ it reduces to the previous case where $W(z,t) = W_o$. An observer travelling with the beam head, i.e., with a velocity $\beta_s c$, sees a backward convective growth of W with a growth length L_g', in the region between the beam head and the point at which W(z,t) reaches its maximum value. In the laboratory frame this growth length is,

$$L_g = \frac{\beta_s c - V_g}{\gamma} . \tag{17a}$$

Although from the laboratory frame of reference the instability grows in time, it is stationary in the region between the peak and the beam head when viewed from the beam head. This is illustrated in figure 5. As a consequence of the backward convective nature of the instability near the beam head, there will be a region in which the effects of the instability are nondestructive, regardless of the length of the device. If the initial perturbation energy density (noise level) is 1% of the beam energy density then it takes about five growth lengths for that perturbation to grow to a level such that W is comparable to the beam energy W_B. Thus a portion of the beam of length $\sim 5L_g$ remains only weakly affected by the instability. Since L_g can be controlled by the experimental parameters this distance can in principle be increased.

(c) $\underline{z < V_g t}$

This is the region between the origin (z=0) and the peak of W(z,t) at $Z = V_g t$. In this region the solution is given by

$$W(z,t) = W_o \exp\left(\frac{\gamma z}{V_g}\right) \tag{18}$$

Here the energy density rises exponentially as a function of z and reaches a peak at $z = V_g t$.

We now apply the solution discussed above specifically to the NRL CPA in the parameter range given in the previous section. From figure 2 we see that the maximum temporal growth rate occurs at $kc/\omega_D = -0.3$ and has a magnitude of $0.486\omega_D$. Also from the plot of ω_r/ω_D we see that the group velocity V_g given by

the slope is roughly 0.0189c. With $\beta_s = 0.906$ the injection velocity in equation (17a) the growth length is 0.61 meters. The diocotron frequency $\omega_D \approx 9 \times 10^8$. Now if the perturbation energy density (i.e., noise level) is 1% of the beam energy density, the ratio $\frac{W}{W_B} \lesssim 1$ for about $5L_g \approx 3$ meters and if the perturbation is 0.01%, then $\frac{W}{W_B} \lesssim 1$ for about $9L_g \approx 5.49$ meters from the beam head (see figure 5). Thus it is possible to successfully accelerate about 3 to 6 meters (depending on the magnitude of the initial perturbation) of the solid beam despite the substantial temporal growth. Also this estimate was done using $\beta_s \sim 0.906$ which is the injection velocity. In figure 6 we use expression 17a to plot L_g against β_s. As the solid beam gets accelerated β_s approaches unity and L_g increases thereby allowing a larger portion of the beam to be unaffected by the transverse instability. Also note that $\omega_D \propto \gamma_h^{-2}$, thus raising the velocity of the hollow electron beam β_h will further increase L_g. Similar treatment can be given for the case of a solid ion beam.

V. Conclusions

The stability of the transverse oscillations for a charged beam propagating through a relativistic hollow electron beam was examined in the parameter regime pertinent to the NRL CPA experiment. The ratio of the beam densities n_s/n_h was maintained as a dependent parameter. For the NRL experiment the ratio of the space charge limited currents $(I_s/I_h) = 0.1$, was used to determine the self consistent n_s/n_h. For a solid electron beam the transverse oscillation had a growth of about $0.5\omega_D$. The growth rate was found to increase with I_s/I_h. This was mainly because increasing I_s/I_h icreased n_s/n_h. The maximum growth rate increased with decreasing β_s . For β_s in the range of -0.5 to -1.0 the growth rate maintains a fairly constant magnitude.

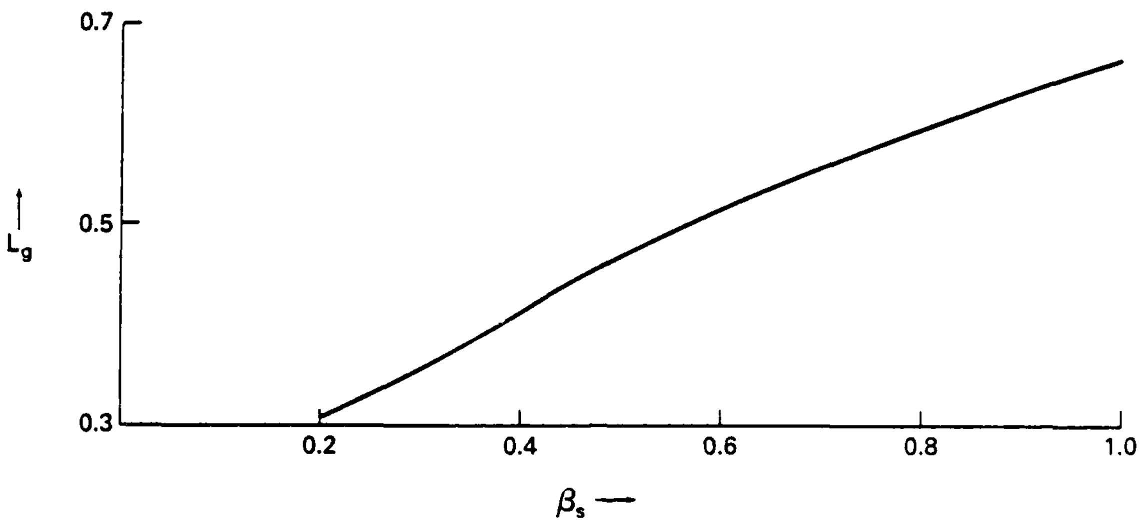

Figure 6 — The magnitude of the growth length L_g, is plotted against the injection velocity of the solid beam, β_s .

Finite geometry effects were examined by solving the wave kinetic equation. It is found that despite the substantial temporal growth rate of the transverse oscillation it is possible to achieve successful acceleration of about 3 to 6 meters of the solid beam length for the present operating parameters. In principle this can be further increased. Thus we conclude that the transverse oscillation will not be fatal to the operation of this device.

A similar conclusion for the case of a solid ion beam can also be made. However it must be pointed out that due to the defocussing of the ion beams this method of propagating a solid ion beam through a relativistic hollow electron beam will fail. Thus the analysis given by Uhm[2] for the solid ion beam acceleration does not apply to the NRL CPA experiment. A solid ion beam will have to propagate through a solid electron beam and this configuration will make a new formalism necessary. A new formalism dealing with the propagation of a solid ion beam through a solid electron beam is now being developed and will be reported in a future paper.

Acknowledgments

We would like to thank Dr. H.S. Uhm of the Naval Surface Weapons Center and Dr. M. Friedman of the Naval Research Laboratory for useful discussions. This work was supported by the Office of the Naval Research.

References

1. Friedman, M., NRL Memorandum Report, 3724 (1978).
2. Uhm, H.S. Phys. Fluids, 25, 1908 (1982).
3. Uhm, H.S, and R.C. Davidson, Phys. Fluids, 23, 813 (1980).

DA

FIL